Food Bioprocess Technol (2008) 1:234–245
DOI 10.1007/s11947-007-0024-z

Acceleration of Maturity of Young Sorghum (Kaoliang) Spirits by Linking Nanogold Photocatalyzed Process to Conventional Biological Aging—a Kinetic Approach

Accelerated Maturation of Young Spirits

**Li-Yun Lin · Chiung-Chi Peng · Hui-Er Wang ·
Chao-Ming Chuang · Tung-Hsi Yu · Kuan-Chou Chen ·
Wen-Ta Chiu · Robert Y. Peng**

Received: 12 May 2007 / Accepted: 11 September 2007 / Published online: 13 October 2007

Abstract With an aim to effectively shorten the ageing period and reduce process cost, a nanogold photocatalyzed process was developed. This process successfully accelerated maturity of young sorghum spirit less than 120 min at ambient temperature. Process parameters relevant to process design were determined to be (1) the amount of acetic acid (≥1.53 g/100 ml); (2) an operation temperature ≤37°C; (3) a degree of mineralization ≤4.87%. Kinetic analysis indicated that to cautiously control dissolved oxygen (DO) to facilitate optimum production of hydroxyl free radical [-OH] could be a crucial step, while the kinetic equations elucidated to indicate production of ethyl acetate and acetic acid could be applicable to reactor scale-up. More importantly, this process provides several benefits including container-saving, space-saving, labor-saving, and no storage-loss due to evaporation; hence, a huge amount of cost reduction (20–24%) in a 4-year aging period could be attainable for each batch cycle.

Keywords Free radical-accelerated maturation · Spirit ageing · Nanogold catalyst · Kinetic analysis

---

L.-Y. Lin · H.-E. Wang
Department of Food and Nutrition,
Hungkuang University,
34, Chung-Chie Rd., Shalu County,
Taichung Hsien 43302, Taiwan

L.-Y. Lin · R. Y. Peng
Research Institute of Biotechnology,
Hungkuang University,
34, Chung-Chie Rd., Shalu County,
Taichung Hsien 43302, Taiwan

C.-C. Peng
Department of Nursing,
Cardinal Tien College of Healthcare & Management,
112, Min-Zu Rd., Sin-Dian,
Taipei County 23143, Taiwan

C.-M. Chuang
Department of Nursing, Hungkuang University,
34, Chung-Chie Rd., Shalu County,
Taichung Hsien 43302, Taiwan

T.-H. Yu
Department and Graduate Institute of Bioindustrial Technology,
Da-Yei University,
Chang Hua, Taiwan

R. Y. Peng (✉)
Research Institute of Medical Sciences, Taipei Medical University,
250, Wu-Xin St.,
Taipei 110, Taiwan
e-mail: ypeng@seed.net.tw

K.-C. Chen
Department of Urology, Taipei Medical University,
250, Wu-Xin St.,
Taipei 110, Taiwan

W.-T. Chiu
Department of Neurosurgery, Taipei Medical University,
250, Wu-Xin St.,
Taipei 110, Taiwan

W.-T. Chiu
Graduate Institute of Injury Prevention and Control,
Taipei Medical University,
250, Wu-Xin St.,
Taipei 110, Taiwan

W.-T. Chiu
Wang-Fang Medical Centre, School of Medicine,
Taipei Medical University,
250, Wu-Xin St.,
Taipei 110, Taiwan

Introduction

Freshly distilled young spirits contain hydrogen sulfides, thiols, thioethers, propanaldehydes, and butenaldehyde. As these compounds usually taste piquant and are unacceptable by consumers, hence, a long ageing period is often required to eliminate these chemicals before sale. For most spirits, ageing process normally takes from 3~5 months to 3~5 years. After aged, they are blended and mixed to gain desired market quality (Ouyang and Chuang 1999; Ouyang et al. 1999; Ouyang and Wu 1999).

Maturation technology may involve: (1) the high-energy maturity methods, (2) the low-energy maturity methods, and (3) a combination of (1) and (2). High energy maturity methods consist of various technologies including UV-irradiation, cobalt (60) irradiation, LASER-irradiation, high frequency treatment, and ultrasonication, whereas low energy maturity technology involves mechanical stirring, vigorous shaking, microwave treatment, heating, and infrared (IR) irradiation (Ouyang and Chuang 1999). Earlier, sweet-fortified wines and spirits were traditionally aged in used (20–80 years old) oak tree barrels to facilitate the diffusion of oxygen. These barrels, often partially filled, were usually stocked in cellars held at desired temperatures (Cutzach et al. 2000). Whereby, oxygen had been considered to play a major role in a variety of chemical reactions occurring during ageing (Cutzach et al. 1999, 2000).

Conventionally, biological ageing is used to be carried out by various types of yeasts such as *Saccharomyces cerevisiae* (Martínez et al. 1995), yet such ageing processes obviously are feasible only for wines with moderate ethanolic concentration (15.5%) and not applicable to those having an alcoholic content >35%. The compositional changes occurring before, during, and after the fermentation process could greatly influence the color and aroma of finished wines (Silva Ferreira et al. 2003). Recent works presented significant information about the chemical compounds associated with "oxidative degradation" of white wines (Escudero et al. 2000a, b, 2002; Ferreira et al. 1997; Silva Ferreira et al. 2002). Oxidation phenomena are generally considered to be favorable and even indispensable for the desired aroma development in sweet-fortified wines (Cutzach et al. 1999, 2000). In reality, the odorant transformation depends on oxygen content entrapped in the wines and the overall extent of oxidation. Substances most characteristic of an accelerated maturity of sweet-fortified red wines are 5-(hyrdoxy-methyl) furfural, acetylformoin, and hydroxymaltol. Their formation is affected by oxidation, while dihydromaltol can only be formed without an oxidative environment (Cutzach et al. 1999). With an aim to shorten the ageing period and enhance the sensory quality of sorghum spirits, we carried out this study using nanogold particles to catalyze the maturation of young sorghum spirits with using UV radiation. The kinetic analysis established that the overall control parameter is the dissolved oxygen (DO). In the presence of which, primary hydroxyl free radicals are generated and used to accelerate a serial chain reaction for spirit maturation process. Such a technology was further evaluated and identified to be an efficient cost-reducing process.

Materials and Methods

Kinetic Analysis

General Photocatalyzed Reaction Mechanism

General photocatalytic reaction mechanisms had been proposed to describe its kinetic aspect (Izumi et al. 1980; Turchi and Ollis 1990; Peng et al. 1997). Typically, a free radical chain reaction may proceed through steps of "initiation", "propagation", and finally end up with "termination".

Initiation

$$\mathrm{Cat} + h\nu(\mathrm{photoenergy}) \rightarrow \mathrm{e}^- + \mathrm{Cat} - \mathrm{h}^+ \tag{1}$$

$$\mathrm{Cat} - \mathrm{h}^+ + \mathrm{H_2O} \rightarrow \cdot\mathrm{OH} + \mathrm{Cat} - \mathrm{h}^+ - \mathrm{H}\cdot \tag{2}$$

$$\mathrm{Cat} - \mathrm{h}^+ - \mathrm{H}\cdot \rightarrow \mathrm{H}^+ + \mathrm{Cat} \tag{3}$$

$$\mathrm{O_2} + \mathrm{e}^- \rightarrow \cdot\mathrm{O_2^-} \tag{4}$$

Where Cat is the nanogold catalysts having a particle size ranging from 80~120 nm, which on exposure to a light source of an approximately 245 nm, can eject electrons e^- from its surface with a simultaneous formation of a "hole, Cat-h^+" (Eq. 1). Both the e^- and Cat-h^+ are very reactive chemical species. The latter may readily produce hydroxyl free radicals ·OH on reaction with water molecules (Eq. 2) to form Cat-h^+–H·, which instantaneously, splits into a hydronium ion H^+ and a native intact Cat (Eq. 3). Alternatively, the electrons e^- released may react with oxygen molecules O_2 to yield superoxide anions $\cdot O_2^-$ (Eq. 4). The overall reaction at the "initiation" stage (Eqs. 1~ 4) is net formation of strong oxidative agents ·OH and $\cdot O_2^-$. In the second stage, generally called "propagation" (not shown), the extremely active oxidizing species superoxide anions $\cdot O_2^-$ (Eq. 4) are capable to induce a series of chain reactions resulting in simultaneous formation of strong secondary oxidants $-HO_2$, $\cdot HO_2^-$ and H_2O_2, provided sufficient supply of oxygen, and high-energy photons are available. Otherwise, the free radical reaction finally would be ceased with the "termination" step:

$$\cdot OH + \cdot OH \rightarrow H_2O_2 \tag{5}$$

$$\cdot OH + H^+ + e^- \rightarrow H_2O \tag{6}$$

As often cited, free hydroxyl radicals are reported to be the most reactive oxidative species (Majlat et al. 1974; Heller and Miline 1978a, b; TNO 1981); thus, the whole sequence of nanogold-catalyzed (Eqs. 1~6) oxidative reactions simply can be simplified as

$$\begin{aligned} &\mathrm{Cat} + \mathrm{Photoenergy} + 17\,H_2O + 17/2\ O_2 \\ &\xrightarrow{k_1} 34\ \cdot OH + \mathrm{Cat} \end{aligned} \tag{7}$$

Mass Balance from the Most Probable Reactions Inside a Reactor for Spirit Ageing

In a reactor process, the high alcoholic content (54%) predominates, while chemical reactions can only proceed with those thermodynamically most favorable intermediate species having the least steric hindrance effect. We arrived at the most probable reactions to demonstrate the spirit maturation by partially referring to the data revealed by GC/MS.

$$2CH_3CH_2OH + 6\cdot OH \xrightarrow{k_2} 2CH_3CO\cdot + 6H_2O \tag{8}$$

$$CH_3CH_2OH + \cdot OH \xrightarrow{k_3} CH_3CH_2O\cdot + H_2O \tag{9}$$

$$CH_3CO\cdot + CH_3CH_2O\cdot \xrightarrow{k_4} CH_3COOCH_2CH_3 \tag{10}$$

$$CH_3CO\cdot + \cdot OH \xrightarrow{k_5} CH_3COOH \tag{11}$$

$$CH_3COOCH_2CH_3 + 18\cdot OH \xrightarrow{k_6} 13H_2O + 4CO_2\uparrow \tag{12}$$

$$CH_3COOH + 8\cdot OH \xrightarrow{k_7} 6H_2O + 2CO_2\uparrow \tag{13}$$

Equations 12 and 13 are commonly called "mineralization". The flow chart to demonstrate the simplified overall equations is illustrated in Fig. 1.

Parallel Consecutive Reaction Kinetics in Nature

Practically, the processors are interested in major reactions that are helpful in upgrading the spirit quality, i.e., to increase the content of esters such as ethyl acetate with some trace amount of carboxylic acids such as acetic acid. Obviously, the mineralization reactions (Equations 12 and 13) are unwanted, yet inevitable. As can be seen, Fig. 1 is parallel consecutive reaction kinetics in nature, i.e., formations of acetic acid and ethyl acetate simultaneously occur.

Steady State Assumption

Following the reaction flow chart (Fig. 1), formation of hydroxyl free radicals resulting from a nanogold photocatalyzed reaction (Eq. 7) can be expressed as

$$d[\cdot OH]/dt = k_1[\mathrm{cat}][h\nu][H_2O][O_2] \tag{14}$$

where [cat] is the effective catalyst surface concentration, [hv] is the photoenergy impinging upon the nanocatalyst gold surface. The consumption rate of hydroxyl free radicals can be obtained from the summation of Eqs. 8, 9, and 11–13. In reality, the reactor virtually contained a vast amount of water compared to that of dissolved oxygen; hence, the term $[H_2O]$ in Eq. 14 can be considered as a constant. Furthermore, because of highly exposed effective surface area of nanogold, the energy (10 W in this case) impinging on the surface of gold powder also technically can be considered as a constant, provided the system is stirred to facilitate complete suspension of nanogold particles. Consequently, both the [energy] and the [Cat] terms in Eq. 14 can also be considered as constants. Thus, Eq. 14 reduces to

$$d[\cdot OH]/dt = k_1{}'[O_2] \tag{15}$$

where $k_1{}' = k_1[\mathrm{cat}][h\nu][H_2O]$ and is called the pseudo-first-order reaction coefficient for conversion of O_2 into hydroxyl free radicals ·OH by such a photocatalyzed reaction.

The consumption rate of hydroxyl free radicals is

$$\begin{aligned} -d[\cdot OH]/dt = [\cdot OH]\{&k_2[CH_3CH_2OH] + k_3[CH_3CH_2OH] \\ &+k_5[CH_3CO\cdot] + k_6[CH_3COOCH_2CH_3] \\ &+k_7[CH_3COOH]\} \end{aligned} \tag{16}$$

At steady state, Eq. 15 = Eq. 16, which leads to

$$\begin{aligned} k_1{}'[O_2] = [\cdot OH]\{&k_2[CH_3CH_2OH] \\ &+k_3[CH_3CH_2OH] + k_5[CH_3CO\cdot] \\ &+k_6[CH_3COOCH_2CH_3] + k_7[CH_3COOH]\} \end{aligned} \tag{17}$$

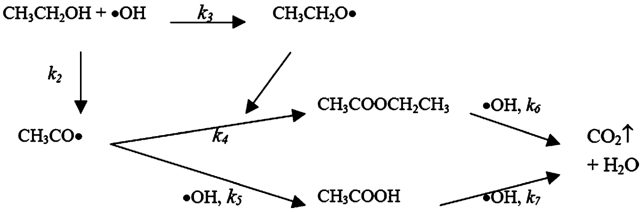

Fig. 1 Simplified overall reaction scheme for maturation process of young Kaoliang spirit by nanogold photocatalyzed reaction

Rearrangement of Eq. 17 gives the concentration of [·OH] at steady state

$$\begin{aligned}[\cdot\mathrm{OH}] = \{&k_1{}'[\mathrm{O_2}]\}/\{k_2[\mathrm{CH_3CH_2OH}] + k_3[\mathrm{CH_3CH_2OH}] \\ &+ k_5[\mathrm{CH_3CO\cdot}] + k_6[\mathrm{CH_3COOCH_2CH_3}] \\ &+ k_7[\mathrm{CH_3COOH\cdot}]\}\end{aligned} \tag{18}$$

The mass balance for ethoxy free radicals involves Eqs. 9 and 10. Its formation rate from Eq. 9 is

$$\mathrm{d}[\mathrm{CH_3CH_2O\cdot}]/\mathrm{d}t = k_3[\mathrm{CH_3CH_2OH}][\cdot\mathrm{OH}] \tag{19}$$

and its disappearance rate (Eq. 10) is

$$-\,\mathrm{d}[\mathrm{CH_3CH_2O\cdot}]/\mathrm{d}t = k_4[\mathrm{CH_3CO\cdot}][\mathrm{CH_3CH_2O\cdot}] \tag{20}$$

Combination of Eqs. 19 and 20 gives the net formation rate of ethoxy free radical, and at steady state

$$k_3[\mathrm{CH_3CH_2OH}][\cdot\mathrm{OH}] = k_4[\mathrm{CH_3CO\cdot}][\mathrm{CH_3CH_2O\cdot}] \tag{21}$$

and

$$[\mathrm{CH_3CH_2O\cdot}] = \{k_3[\mathrm{CH_3CH_2OH}][\cdot\mathrm{OH}]\}/k_4[\mathrm{CH_3CO\cdot}] \tag{22}$$

Alternatively, Eq. 8 gives the formation rate of acetoxy free radical as:

$$\mathrm{d}[\mathrm{CH_3CO\cdot}]/\mathrm{d}t = k_2[\mathrm{CH_3CH_2OH}][\cdot\mathrm{OH}] \tag{23}$$

The elimination rate of acetoxy free radical can be calculated from the sum of Eqs. 10 and 11,

$$-\mathrm{d}[\mathrm{CH_3CO\cdot}]/\mathrm{d}t = [\mathrm{CH_3CO\cdot}]\{k_4[\mathrm{CH_3CH_2O\cdot}] + k_5[\cdot\mathrm{OH}]\} \tag{24}$$

and at steady state with Eq. 23=Eq. 24, we have

$$\begin{aligned}&k_2[\mathrm{CH_3CH_2OH}][\cdot\mathrm{OH}] \\ &\quad = [\mathrm{CH_3CO\cdot}]\{k_4[\mathrm{CH_3CH_2O\cdot}] + k_5[\cdot\mathrm{OH}]\}\end{aligned} \tag{25}$$

On rearrangement of Eq. 25, we have the steady state concentration of acetoxy free radical

$$[\mathrm{CH_3CO\cdot}] = \{k_2[\mathrm{CH_3CH_2OH}][\cdot\mathrm{OH}]\}/\{k_4[\mathrm{CH_3CH_2O\cdot}] + k_5[\cdot\mathrm{OH}]\} \tag{26}$$

Substitution of Eq. 26 into Eq. 22 yields

$$[\mathrm{CH_3CH_2O\cdot}] = [(k_3k_5)/k_4(k_2 - k_3)][\cdot\mathrm{OH}] \tag{27}$$

As mentioned, in this process, the main products of interest being really beneficial to taste and aroma or flavor are acetic acid and ethyl acetate.

The net formation rate of ethyl acetate $\mathrm{CH_3COOCH_2CH_3}$ as shown in Fig. 1 is

$$\begin{aligned}&\mathrm{d}[\mathrm{CH_3COOCH_2CH_3}]/\mathrm{d}t \\ &\quad = k_4[\mathrm{CH_3CO\cdot}][\mathrm{CH_3CH_2O\cdot}] - k_6[\cdot\mathrm{OH}] \\ &\qquad \times [\mathrm{CH_3COOCH_2CH_3}]\end{aligned} \tag{28}$$

While the net formation rate of acetic acid is

$$\mathrm{d}[\mathrm{CH_3COOH}]/\mathrm{d}t = [\cdot\mathrm{OH}]\{k5\{[\mathrm{CH_3CO\cdot}] - k_7[\mathrm{CH_3COOH}]\} \tag{29}$$

Production rate of ethyl acetate Substitution of Eqs. 26 and 27 into Eq. 28 yields

$$\begin{aligned}&\mathrm{d}[\mathrm{CH_3COOCH_2CH_3}]/\mathrm{d}t \\ &\quad = k_2\{k_4[\mathrm{CH_3CH_2OH}][\cdot\mathrm{OH}]\}/\{k_4[\mathrm{CH_3CH_2O\cdot}] + k_5[\cdot\mathrm{OH}]\} \\ &\qquad \times \{(k_3k_5/k_4)[\cdot\mathrm{OH}]/[(k_2 - k_3)]\} \\ &\qquad - k_6[\cdot\mathrm{OH}][\mathrm{CH_3COOCH_2CH_3}]\end{aligned} \tag{30}$$

Substitution of Eq. 27 into Eq. 30 leads to the net formation rate of ethyl acetate

$$\begin{aligned}&\mathrm{d}[\mathrm{CH_3COOCH_2CH_3}]/\mathrm{d}t \\ &\quad = [\cdot\mathrm{OH}]\{k_2k_3k_5[\mathrm{CH_3CH_2OH}]/[(k_3k_5) + (k_2 - k_3)k_5] - k_6[\mathrm{CH_3COOCH_2CH_3}]\}\end{aligned} \tag{31}$$

Production rate of acetic acid Substitution of Eq. 26 into Eq. 29 we have the net formation rate for acetic acid

$$\begin{aligned}&\mathrm{d}[\mathrm{CH_3COOH}]/\mathrm{d}t{=}(k_2{-}k_3)[\cdot\mathrm{OH}] \\ &\quad \times [\mathrm{CH_3CH_2OH}]{-}k_7[\mathrm{CH_3COOH}]\}\end{aligned} \tag{32}$$

Consumption rate of ethanol The consumption rate for ethanol is

$$-\,\mathrm{d}[\mathrm{CH_3CH_2OH}]/\mathrm{d}t = -(k_2 + k_3)[\mathrm{CH_3CH_2OH}][\cdot\mathrm{OH}] \tag{33}$$

Mineralization rate Finally, the mineralization rate in this system is

$$\begin{aligned}&\mathrm{d}[\mathrm{CO_2}]/\mathrm{d}t = k_6[\cdot\mathrm{OH}] \\ &\qquad \times \{[\mathrm{CH_3COOCH_2CH_3}] + k_7[\mathrm{CH_3COOH}]\}\end{aligned} \tag{34}$$

Source of Spirits

Young spirits, the white distilled brand of sorghum spirits made from steam-cooked sorghum (Kaoliang) by a serial processes involving inoculation, fermentation, and distillation at solid phase and aged for 1 month were provided by Taiwan Tabacco and Liquor. Its alcoholic content was 54% *w*/*v*.

Authentic Volatile Compounds

The authentic odorants used in this experiment supplied by Aldrich. (UK) had purity at least 97% when measured by gas chromatography Angilent HP-6890. The column used was DB-1 capillary column (ℓ =60 m; id=0.25 mm) in which was packed with Chrompack fused silica (thickness= 0.32 μm). The detector used was of type FID (Angilent 6890, Willington, De, USA).

Reactor Installation

A three-necked 5 l reactor was installed with an UV light source (10 W, effective wavelength, 245 nm) at the central axis. The other two necks were installed with a thermocouple (sensitivity, within 0.01°C) and a pH meter (sensitivity within 0.1 U), respectively. In each batchwise operation, the reactor was filled with 3.0 l of Yusan Kaoliang spirits sample and 19.8 mg of nanogold powders (85.6% smaller than 100 nm, size ranging from 80~120 nm), which were homogeneously suspended in the reactor with a magnetic stirrer during the operation. Each batchwise reaction was carried out at ambient temperature. The head space of the reactor was always kept at 2.0 l above the liquid level. The initial dissolved oxygen (DO) was 6.7 ppm.

Recovery of nanogold particles When reaction is completed, nanogold powder can be easily recovered simply by sedimentation. The recovery rate reached 100%. On ceasing agitation, the nanogold particles readily sediment to the bottom of reactor within a few minutes without any further treatment of either centrifugation or filtration.

Determination of Ethanolic Content

Ethanolic content was determined following the method of Zoecklein et al. (1990). Sample spirits (10 ml) was measured accurately and added with 1 ml of acetonitrile as the internal standard, and filtered with a Millipore filter (0.45 μm in porosity. GC analysis was carried out with a gas chromatography (Gas chromatography Angilent HP-6890). The column used was DB-1 capillary column (ℓ= 60 m; id=0.25 mm, thickness=1 μm) packed with chromopack-fused silica. The detector used was of type FID (Angilent 6890, Willington, De, USA). Nitrogen gas was used as the carrier gas operated at a flow rate of 1 ml/min with a split rate of 60:1. The GC oven temperature initially was held at 40°C for 10 min and raised from 40 to 240°C in 30 min at 2°C/min and maintained at 240°C for 10 min. The temperature at injection port was held at 200°C, and that at detector, was held at 220°C.

Assay of Volatile Compounds by GC-Mass Spectrometry

The odorants in spirits were analyzed with method of Romer and Renner (1974). Spirit sample (30 ml) was diluted with distilled water to a concentration of 4% alcoholic content (sample A), added with 2 ml of internal standard (16.9 mg of cyclohexanol accurately weighed and dissolved in 100 ml of distilled water). Sample A (30 ml) was transferred into an Erlenmeyer flask (250 ml). Dichloromethane (120 ml) was added with vigorous stirring for 2 h, let stand for separation of the two layers, and separated with a separation funnel to obtain the lower dichloromethane layer. The latter was added with a sufficient amount of anhydrous sodium sulfate, shaken vigorously, and filtered through a filter paper into an oval-shaped flask. The oval flask was placed at the bottom of the concentration tower and heated at 45°C using a constant temperature water bath. The first stage concentration was proceeded until 1~2 ml remained in the flask. The second stage concentration was continued with nitrogen gas blowing at a flow rate of 25 ml/min to obtain the residual odorant concentrate 0.5 ml (sample B). The sample B obtained in the above was directly injected into gas chromatography/mass selective detector (GC-MSD)

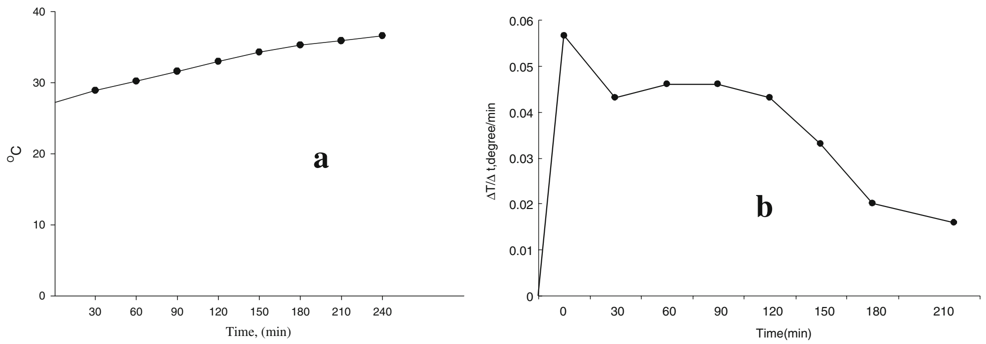

Fig. 2 Reaction temperature profile vs time in maturation process of young Yusan Kaoliang spirit by nanogold photocatalyzed process. **a** A common T-t profile: Young Yusan Kaoliang spirit 3,000 ml. Nanogold catalyst 19.8 mg. UV source (10 W): 245 nm. Reaction time 4 h at ambient temperature 27.8°C with magnetic stirring. **b** The first derivative presentation of (**a**): peak exothermic time occurred at 15 min and the second maximum at 110 min after the start of reaction

Table 1 Reaction parameters obtained[a]

Item	Reaction phase			
Reaction parameter	Phase 1	Phase 2	Phase 3	Phase 4
TOC				
Time period, min	0–60	60–90	90–150	150–240
Rate coefficient (g/l min)	–0.1167	–0.3333	–0.0333	–0.1833
TIC				
Time period, min	0–30	30–210	210–240	Lacking
Rate coefficient, (g/L-min)	0.1467	0.0233	0.0067	Lacking
Max exothermic time, min	15 (1st max)	–	110 (2nd max)	–
Min pH (time, min)	3.4 (60)	3.4 (60)	–	–

During the photocatalyzed oxidation, some intermediate aroma could be produced from transformation of ethanol (organic carbon). However, the free radical reaction was proceeding continuously so that the extreme final product CO_2 (inorganic carbon) would be eventually accumulated in the reaction mixture. Literally, such a phenomenon is called "mineralization".

[a] Yusan Kaoliang wine 3000 ml. Nanogold catalyst 19.8 mg; UV source (10 W): 245 nm. Reaction time 4 h at ambient temperature 27.8°C with magnetic stirring.

Table 3 Results of sensory evaluation on the Yusan Kaoliang spirits as a time function during the nano-photocatalyzed maturation[a]

Sample reaction time (min)	Aroma	Taste	Overall preference
0	[b]6.00[a]±0.52C	6.00±0.68C	6.00±0.72C
30	6.06±0.34C	6.18±0.22C	6.35±1.02BC
60	6.29±0.82BC	6.06±0.46C	6.24±0.44BC
90	6.88±1.22ABC	6.82±0.65ABC	6.71±1.02ABC
120	7.47±0.55A	7.43±0.42A	7.49±0.38A
150	7.35±0.89A	7.18±0.68A	7.29±0.24A
180	6.82±0.44ABC	7.00±0.78AB	6.76±0.45ABC
210	6.66±0.24ABC	6.71±0.64ABC	6.72±0.44ABC
240	6.10±0.56C	6.15±0.47C	6.08±0.48C

[a] Yuasn Kaoliang spirit 3,000 ml. Nanogold catalyst 19.8 mg. UV source (10 W): 245 nm. Reaction time: 4 h at ambient temperature 27.8°C with magnetic stirring. Sampling was conducted every 30 min. The results of acceptance were tested through the use of a nine-point Hedonic scale (International Organization for Standardization 1987).

[b] Average of 24 judgments. Hedonic Scale (9) = like extremely; (5) = neither like nor dislike; (1) = dislike extremely. Data are expressed in Mean ± SD from three different individual experiments. Means with different capital letters within the same row are significantly different ($p<0.05$)

(Hewlett-Packard 6890, connected to Hewlett-Packard 5973 MSD). A capillary column (column type DB-1: 60 mm in length with id=0.25 mm) was used. Carrier gas helium gas was operated at a flow rate of 1.0 ml/min with a split ratio of 80:1. The temperature was programmed starting from an initial at 40°C for 10 min, by 2°C/min to 240°C and remained for 30 min. The injector temperature was set at 250°C. The MS source temperature was 230°C, the EM voltage was adjusted to 1,800 V, and the MS Quad temperature was 150°C.

The qualitative and quantitative determination of odorant components was performed following the method of Majlat et al. (1974). The odorant components in Kaoliang spirit was cross referred to the diagrams obtained from the GC-MSD. The triplicate quantitative determinations were carried out using an internal standard. The concentration of a specific component C was calculated from Eq. 35.

$$C = (A_s/A_{in}) \times (C_{st}) \tag{35}$$

where C is the ppm of the specified component;

A_s is the area of integrated diagrams obtained from GC-MS for the sample;
A_{in} is the area of integrated diagrams obtained from GC-MS for the internal standard; and
C_{st} is ppm of internal standard

The structural determinations were processed by referring to the computerized database of Heller and Miline

Table 2 Degree of mineralization during the nano-photocatalytic maturation process of young Kaoliang spirits[a]

Parameter	Time (min)								
	0	30	60	90	120	150	180	210	240
TOC, g/l	261.37	256.55	255.45	245.75	244.57	244.18	238.56	235.00	226.74
TIC, g/l	7.81	12.23	12.45	13.96	14.20	15.05	15.58	16.58	16.74
%DM[b]	2.68	4.2	4.27	4.79	4.87	5.17	5.35	5.69	5.75

As a consequence of the photocatalyzed free radical oxidation of ethanol, the extreme final product CO_2 (inorganic carbon) would be eventually accumulated in the reaction mixture. Such a phenomenon is termed as "mineralization". The ratio of TIC/TOC is defined as the degree of mineralization.

[a] Yusan Kaoliang wine 3000 ml. Nanogold catalyst 19.8 mg; UV source (10 W): 245 nm. Reaction time 4 h at ambient temperature 27.8°C with magnetic stirring.

[b] *% DM* Degree of mineralization = $[(\mathrm{TIC}) / (\mathrm{TOC})_o] \times 100\%$

Table 4 Odorant transition profile during nano-photocatalytic maturation of young Kaoliang (Sorghum) spirits*

Number	Compound	Reaction time (min)								
		0	30	60	90	120	150	180	210	240
		Concentration (ppm)								
1	(2.2-diethoxyethyl)-benzene	4.7	4.2	3.94	–	3.7	2.9	–	2.9	2.7
2	1-(1-ethoxyethyl)-propane	0.7	0.9	0.62	0.7	0.8	0.5	0.5	0.5	0.7
3	1-(1-ethoxyethyl)-pentane	1.2	1.1	0.9	0.76	0.8	1.0	1.1	1.1	1.6
4	1.1.3.3-tetraethoxy-propane	–*	–	+ *	–	–	–	–	+	+
5	1.1.3-triethoxy butane	1.2	1.3	1.2	2.0	1.4	1.5	1.4	2.5	1.7
6	1.1.3-triethoxy propane	6.3	5.9	5.6	5.8	5.2	4.7	5.8	4.5	4.5
7	1.1-diethoxy ethane	62.9	112.8	82.9	62.1	112.6	39.2	66.8	24.8	59.6
8	1.1-diethoxy-3-methyl-butane	8.0	9.3	5.3	5.5	5.4	3.8	5.0	4.2	4.8
9	1-butanol	0.7	0.9	0.9	1.3	0.8	–	1.1	–	1.3
10	2.4.5-trimethyl-1.3-dioxolane	1.0	2.6	1.6	1.5	2.5	1.0	1.1	0.7	1.8
11	2-butanol	13.2	7.	7.0	5.1	–	3.8	3.8	2.9	0.2
12	2-methoxy-4-methyl phenol	2.1	–	–	–	–	–	–	–	–
13	2-methyl-1-butanol	20.2	–	20.1	–	18.8	–	10.8	–	4.1
14	2-methyl-2-butanol	–	0.2	–	0.1	0.2	0.3	+	–	–
15	3-methyl butanol	–	0.6	0.4	0.4	0.7	0.2	0.3	0.1	0.6
16	4-ethyl-2-methoxy phenol	3.6	0.8	–	–	–	–	–	–	–
17	5-methyl furfural	–	–	–	–	–	+	+	+	+
18	9.9-diethoxy ethyl nonanoate	0.9	0.7	0.3	0.6	1.0	0.4	0.5	0.4	0.4
19	Acetoin	7.4	10.9	4.8	10.4	8.9	1.7	7.7	1.2	7.3
20	Acetic acid	+	0.6	+	2.5	2.00	1.3	1.9	0.4	2.0
21	Amyl acetate	3.1	3.7	2.8	3.1	0.8	2.5	3.0	2.3	2.2
22	Benzaldehyde	–	0.7	+	0.8	+	+	+	0.6	0.4
23	Benzeneacetaldehyde	2.3	3.7	3.9	6.6	3.9	3.4	5.9	2.9	4.6
24	Cyclohexene	–	2.4	3.2	1.6	–	1.4	–	0.4	–
25	Decanoic acid	–	0.5	–	1.4	0.5	0.9	–	–	–
26	Diethyl succinate	16.5	14.6	14.1	15.2	13.8	11.5	14.6	11.6	11.4
27	Dihydro-5-pentyl 2(3H)-furanone	–	–	+	+	0.4	0.6	0.6	0.7	0.6
28	Ethyl linoleinate	8.7	+	2.8	–	2.0	+	1.9	0.4	+
29	Ethyl palmitate	207.5	128.7	63.1	–	–	54.8	44.4	–	17.4
30	Ethyl 2-hydroxy-3-phenylpropanoate	1.7	0.8	1.3	1.6	1.2	0.9	1.1	1.0	0.8
31	Ethyl 2-methylbutyrate	–	–	+	0.5	–	+	–	–	0.3
32	Ethyl 9-oxo-nonanoate	–	0.8	0.8	1.2	0.9	0.7	0.8	0.8	0.6
33	Ethyl acetate	26.0	37.5	34.6	18.3	59.6	9.6	20.1	5.2	15.7
34	Ethyl benzoate	–	0.5	+	0.3	+	0.4	0.5	0.5	0.4
35	Ethyl butyrate	3.8	7.4	5.3	5.2	6.2	0.3	3.5	3.2	5.3
36	Ethyl caprylate	22.6	24.0	21.2	22.7	19.0	16.46	18.6	17.4	17.8
37	Ethyl cinnamate	–	–	–	–	–	+	+	+	+
38	Ethyl decanoate	3.3	4.4	–	2.1	2.0	2.9	2.9	2.0	1.3
39	Ethyl isobutyrate	–	1.1	0.7	0.7	0.9	0.4	0.5	+	0.7
40	Ethyl isovalerate	–	–	+	0.5	0.5	+	0.4	–	0.5
41	Ethyl lactate	373.4	399.9	377.9	354.1	351.1	253.4	326.6	232.7	257.1
42	Ethyl laurate	3.1	2.3	+	+	0.7	1.5	0.8	–	0.4
43	Ethyl linoleate	161.6	–	41.7	+	32.0	+	23.	–	8.6
44	Ethyl myristate	6.0	3.9	1.6	+	+	1.6	1.2	–	0.5
45	Ethyl nonanoate	0.9	0.9	0.7	0.7	0.6	0.7	0.8	0.7	0.5
46	Ethyl octanoate	9.0	7.7	7.3	7.7	6.6	6.2	7.4	5.7	5.4
47	Ethyl propanoate	2.1	3.9	3.7	3.2	5.7	1.9	2.4	1.1	4.3
48	Ethyl stearate	7.2	10.3	1.8	0.9	1.5	2.0	1.3	1.3	0.5
49	Ethyl valerate	–	0.8	0.5	0.6	0.5	+	0.5	0.6	0.5
50	Ethyl-2-hydroxycaproate	19.8	18.0	17.7	18.5	16.5	14.4	18.8	13.6	13.6
51	Ethylphenyl acetate	–	0.9	0.8	0.8	0.7	0.7	0.8	0.8	0.6
52	Furfural	72.6	–	4.7	+	3.8	+	+	–	–

Table 4 (continued)

Number	Compound	Reaction time (min)								
		0	30	60	90	120	150	180	210	240
		Concentration (ppm)								
53	Heptanol	–	–	1.9	–	1.8	+	+	–	+
54	Hexanal	–	0.6	+	0.5	0.5	+	0.2	–	0.4
55	Hexanoic acid	–	3.2	7.0	–	6.5	–	0.6	+	2.4
56	Hexanol	–	2.0	1.7	2.0	1.3	1.1	2.0	–	1.4
57	Isoamyl acetate	3.3	4.6	3.5	4.2	3.7	3.5	3.3	5.0	3.7
58	Isoamyl alcohol	87.7	112.2	114.6	106.1	89.0	81.1	87.7	14.8	80.1
59	Isobutyl acetate	–	0.8	0.5	0.7	0.7	0.1	0.5	0.4	0.9
60	Isobutyl alcohol	1.6	4.6	4.5	2.4	4.1	1.3	2.1	0.3	1.5
61	Linoleic acid	13.5	9.5	–	–	–	5.0	2.6	0.6	0.5
62	Methyl oleate	103.6	90.9	–	–	25.5	–	20.9	–	2.8
63	Myristic acid	0.9	0.7	+	–	+	–	0.5	0.3	+
64	Octanoic acid	–	3.1	2.2	0.8	0.7	+	2.1	0.1	1.1
65	Octanol	–	0.4	0.5	0.7	0.6	0.8	0.7	0.7	0.6
66	Oleamide	68.1	+	13.4	5.8	8.0	4.9	7.5	3.9	5.2
67	Oleic acid	21	10.6	–	–	–	5.5	4.2	–	1.5
68	Palmitic acid	51.7	37.0	19.6	–	–	17.8	9.9	–	2.8
70	Phenylethyl acetate	2.2	2.2	2.0	2.5	2.0	1.8	2	1.9	1.8
71	Propanoic acid	–	–	0.4	–	0.3	–	0.2	–	–
72	Propyl acetate	9.8	2.5	1.8	0.2	2.4	0.7	1.1	0.4	1.7
73	Tetramethyl pyrazine	–	0.6	0.6	–	0.5	0.5	–	0.4	0.3

*Yusan Kaoliang wine 3000 ml. Nanogold catalyst 19.8 mg; UV source (10 W): 245 nm.
Reaction time 4 h at ambient temperature 27.8°C with magnetic stirring.
– Undetectable, + trace amount only

(1978a, b) and TNO (1981). Alternatively, some data were referred to the cited mass spectroscopic data.

Reaction Temperature Profile

The reaction temperature was taken manually every 5 min from the beginning of turn-on of the UV source.

Acidity and PH Profiles

The pH values were directly read from the pH meter attached in the reactor. The volatile acidity was determined according to Amerine and Ough (1980).

Ten milliliters of the sample was transferred into a Sellier tube. The mixture was heated to initiate the steam to be purged into the tube. The volatile components were thus driven out and condensed into the receiver. The solution in the receiver was moderately heated to boil for a period no longer than 30 s. Phenolphthalein indicator (three drops) was added while hot. The mixture was titrated against 0.1 N NaOH to the endpoint (pinkish color). Volatile acid content was calculated according to Eq. 36.

$$C_{\mathrm{va}} = (V)\cdot(N)\cdot(6)/\cdot S \qquad (36)$$

where C_{va} is the volatile acid content expressed as grams acetic acid per 100 ml; V is the volume of titrant NaOH (ml); N is the equivalent of NaOH; S is the volume of sample (ml).

Sensory Evaluation Studies

The results of acceptance were tested through the use of the seven-point Hedonic Scale (International Organization for Standardization 1987; (Silva Ferreira et al. 2003). A total of 24 wine masters evaluated the product with respect to overall all “like” or “dislike”. Data are expressed as mean score with 1—extremely dislike; 5—neither like nor dislike; 9—extremely like. (N=24).

Safety Tests

Acute toxicity test was performed for 7 days by Japan Food and Safety Examination Bureau. Female Spraque—Dawley (SD) rats SPF, aged 6 weeks, were used for safety tests. Their body weights were measured before experiment and before killing, respectively. The aged spirits were fed to SD per os with a single dose of 4 ml/kg. Their growth status was recorded daily.

Statistical Methods

The statistical significance of the differences among samples tested was analyzed using Statistical Analysis System (SA System) software. Student's *t* test was performed. Differences were considered to be significant at level of $p<0.05$. Results are presented as mean ± SD within triplicate results of each experiment.

Results and Discussion

Free radical catalyzed reaction was exothermic in nature (Fig. 2a and b). With sufficient amount of dissolved oxygen (DO=6.7 ppm at the initial point), the reaction vigorously proceeded with a large amount of heat evolved between 15 and 30 min after the start of reaction (Table 1 and Fig. 2b). The oxidative degradation reaction of ethanol and its intermediate oxidized products proceeded rapidly. Total organic carbons (TOC) decreased from 262 to 227 g/l with concomitant formation of total inorganic carbons (TIC) from 7.8 to 16.6 g/l within 240 min (Table 2). Obviously, although mineralization (reactions k_6 and k_7) is inevitable, it is, however, controllable.

Sensory evaluation studies (Table 3) showed that an optimum product was obtainable between 90 to 120 min after the beginning of the reaction (CL: 0.95, n=48), which virtually and relevantly associated with the change in odorant transition profile (Table 4) and the acidity (1.18 g/100 ml; pH 3.4) of the final product (Table 2). Some 70 odorants were examined, the acetic acid content was found approaching maximum at 90 min with slight decrease to 2.00 ppm at 120 min after the beginning of the reaction (Table 4). Simultaneously, the concentration of ethyl acetate increased to the highest peak of 59.61 ppm at 120 min (Table 4). Other important flavor component levels at 120 min were, respectively, 112.57, 18.77, 0.71 and 8.89 for 1,1-diethoxy ethane, 2-methyl 1-butanol, 3-methyl butanol, and acetoin, respectively (Table 4). As for common good esters, the contents of which at 120 min were 13.18,

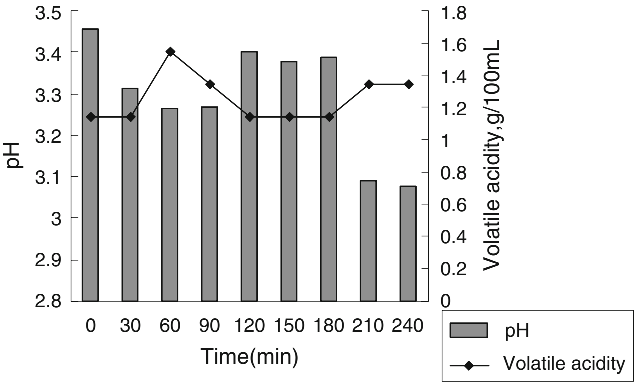

Fig. 3 Acid production vs reaction time in maturation process of young Yusan Kaoliang spirit catalyzed by nanogold photocatalyzed process. Young Yusan Kaoliang spirit 3,000 ml. Nanogold catalyst 19.8 mg. UV source (10 W): 245 nm. Reaction time 4 h at ambient temperature 27.8°C with magnetic stirring. During the photocatalyzed oxidation, some intermediate aroma could be produced from transformation of ethanol (organic carbon). Acid production occurs at a reaction time only shortly before mineralization. As shown, peak acid production time occurred at 60 min post the start of reaction

Table 5 Body weight variations of SD rats SPF prior to and post administration of the maturity accelerated young Kaoliang spirits[a]

Rat number	Before fed B. Wt. (g)	Before killing B. Wt. (g)	Wt. increment g
1	227.9	267	39.1
2	224.1	240.3	16.2
3	222.2	262.4	40.2
4	228.4	248.2	19.8
5	215	220.4	5.4
Mean ± SD	222.3±5.42	247.66±18.63	20.14±15.12
1	221	250.5	29.5
2	213.7	241.1	27.4
3	233.1	261.6	28.5
4	227	250.4	23.4
5	228	285.6	57.6
Mean ± SD	224.56±7.44	257.84±17.13	33.28±13.79
1	207.8	229.3	21.5
2	216.8	237.7	21
3	23	261	30
4	223.4	242.8	19.4
5	207.1	236.8	29.7
Mean ± SD	217.2±10.24	241.52±11.91	24.32±5.11
1	217.9	237.8	19.9
2	210.8	233	22.2
3	214	227.3	13.3
4	212.3	253.8	41.5
5	207	221.9	14.9
Mean ± SD	212.4±4.02	234.76±12.21	22.36±11.29
1	220.5	230.4	9.9
2	219.4	239.2	19.8
3	213	225.4	12.4
4	213.2	247.2	34
5	206.4	240.8	34.4
Mean ± SD	214.5±5.69	236.6±8.67	22.1±11.63
1	216.5	237.2	20.7
2	220	233.2	13.2
3	208.2	232	23.8
4	225.8	227.8	2
5	213.4	218.1	4.7
Mean ± SD	216.78±6.65	229.66±7.28	12.88±9.56

[a] Expressed in Mean ± SD, analyzed statistically by Student *t* test. Acute toxicity test was performed for 7 days by Japan Food and Safety Examination Bureau. Female Sprague–Dawley Rats SPF, aged 6 weeks, were used for safety tests. Their body weights were measured before the experiment and before killing, respectively. The aged spirits were fed to SD per os with a single dose of 4 ml/kg. Their growth status was recorded daily.

Table 6 Biochemical examinations of the rat blood obtained from the acute toxicity test[a]

Rat number	SGO-T	SGP-T	BUN
1	132	40	19.4
2	525	77	18.9
3	238	52	20.2
4	96	57	16
5	123	135	18
Mean ± SD	222.8±177.37	72.2±37.56	18.5±1.61
1	228	35	29.5
2	94	29	27.4
3	128	25	28.5
4	182	31	23.4
5	188	33	57.6
Mean ± SD	164±52.09	30.6±3.85	17±1.43
1	184	229.3	21.5
2	53	237.7	21
3	114	261	30
4	100	242.8	19.4
5	84	236.8	29.7
Mean ± SD	107±48.66	26.4±5.08	17.62±1.80
1	231	32	15.1
2	88	20	18.6
3	125	28	17.5
4	173	41	20.3
5	178	31	20.2
Mean ± SD	159±54.63	30.4±7.57	18.34±2.15
1	83	230.4	9.9
2	129	239.2	19.8
3	109	225.4	12.4
4	124	247.2	34
5	231	240.8	34.4
Mean ± SD	135±56.46	34.8±7.29	15.34±2.39
1	174	44	16.7
2	197	41	14.6
3	102	25	21.2
4	152	43	15
5	77	23	12.8
Mean ± SD	140.4±49.90	35.2±10.31	16.06±3.19

[a] Expressed in mean ± SD, analyzed statistically by Student *t* test. Acute toxicity test was performed for 7 days by Japan Food and Safety Examination Bureau. Female Spraque–Dawley Rats SPF, aged 6 weeks, were used for safety tests. Their body weights were measured before the experiment and before killing, respectively. The aged spirits were fed to SD per os with a single dose of 4 ml/kg. Their growth status was recorded daily.

18.98, 351.05 16.53, 0.74, 3.66, and 2.39 ppm for ethyl succinate, ethyl caprylate, ethyl lactate, ethyl-2-hydroxycaproate, ethylphenyl acetate, isoamyl acetate, and propyl acetate, respectively. Although not all at their maximum values at 120 min post the start of reaction, they still remained at relatively high levels (Table 4). The volatile acidity reached its maximum value of 1.53 g/100 ml at 60 min, while pH value remained at its lowest point of 3.4 (Fig. 3; Table 1), indicating vigorous oxidative degradation was proceeding in the reactor during 0–60 min.

Seemingly, a regular rule could be found from Table 4. Results in Table 4 evidenced active formation of ethyl-, ethoxy-, and acetoxy free radical groups as the intermediates during the oxidative reaction course. Consequently, these functionality-containing compounds all exhibited damping profiles during the reaction. In contrast, those compounds that did not bear such functionality were degraded all the way down (Table 4). Acetic acid has always been considered to be the most important volatile acid resulting from ageing process; the fixed and volatile acid content for 1-year aged wines commonly may be only 4.37 and 18.21%, respectively; however, an 80-year aged distilled wine was reported to contain 127.55 and 265.5% (data converted to g/100 l of 100% alcohol content), respectively (Ouyang et al. 1999). Steady and tender ageing can improve ester contents from 0.148 to 0.190 g/100 ml and that of total acid from 0.036 to 0.06 5 g/100 ml in distilled wines. Nonetheless, it is advisable to avoid excess vigorous oxidation (Ouyang et al. 1999; Silva Ferreira et al. 2002; Cutzach et al. 1999). Over oxidation may result in “acid odor” in maderized wines (Cantarelli 1967). In the case with dry wines, these phenomena may lead to deterioration of the bouquet ageing.

Although esterification index has long been accepted as a criterion in wine ranking (Ouyang et al. 1999), it would not be applicable to a photocatalyzed maturation process. Instead, a

Table 7 Cost saving analysis[a]

Item	Extra-cost due per year (%)	Extra cost due for 4-year ageing (%)	Nano Tech Maturation
Barrels used for storage	1.0	4	Not required
Stock house/ Rent for stock house	1.0	4	Not required
Transportation workers’ pay/ Management charge	2	8	Not required
Evaporation loss during aging	2–3	8–12	Unlikely to happen
Catalyst gold (80–120 nm)[a]	–	–	Initially can be a big item of cost (6.6 mg/L); yet 100% is recoverable[a].
Total cost		24–28%	

[a] Courtesy of Taiwan Tabaco and Wines Monopoly Bureau: generally, young spirits need at minimum 4 years to get aged.

[b] Nanogold powder (80–120 nm) can be a large burden, yet it is 100% recoverable. As without stirring, they readily sediment without any operation of centrifugation or filtration.

new balance of the constituting flavors produced in such a reaction would play an important role in determining the sensory quality. Hence, to control the oxygen content is obviously a crucial technology in accelerating the maturity (Ouyang et al. 1999; Silva Ferreira et al. 2002; Cutzach et al. 1999). In other words, a novel ranking parameter is required for such an evaluation. Maria Andre et al. (2004) indicated a tendency of aldehydes increase and lowering of fuel oil levels during the ageing period. In addition to increased values of ethyl acetate and acetic acid, other changes probably are related to better sensory quality of aged sugar cane spirits (Maria Andre et al. 2004).

By using the nanogold photocatalysis, the spirit successfully accelerated the maturity of the young spirits with pleasant sensory feeling. Interestingly, the product obtained by the maturity-acceleration technique virtually was comparable to conventionally aged products with regard to its quality (Table 3). More importantly, the matured product was concomitantly identified to be nontoxic (Tables 5 and 6).

Practically, we are only interested in the major reactions that are helpful in upgrading the quality of the spirit, i.e., to increase the content of esters such as ethyl acetate with some trace amount of carboxylic acids such as acetic acid. Obviously, the mineralization reactions (Eqs. 30 and 31) are unwanted, yet inevitable. According to the kinetic analysis, the overall reaction was parallel consecutive reaction kinetics in nature (Fig. 1), i.e., the hydroxyl free radical (·OH) catalyzed formation of ethyl acetate, and acetic acid virtually is a parallel consecutive kinetics.

The free radical initiated chain reactions are characteristically difficult to estimate with their reaction kinetics. Kinetically, at initial stage of reaction, in the presence of large amounts of ethanol, the amounts of ethyl acetate and acetic acid present are very small compared to the mother substrate ethanol; hence, the rate constants k_6 and k_7 (Fig. 1) are negligible, and the original parallel and consecutive reaction can be treated as a pseudo-parallel or simultaneous kinetic. As elucidated in this present manuscript, the entire process can be mainly affected by the hydroxyl free radical concentration [·OH] (Eqs. 14, 15 and 18). Given a constant light intensity with definite geometry (Eq. 14), a constant particle size of nanogold catalyst in a well-suspended solution (Eq. 14), the concentration of [·OH] was merely proportional to the dissolved oxygen (DO) (Eq. 18). To optimize or enrich ethyl acetate (Eq. 31) and acetic acid (Eq. 32) that are pleasant to the human sensors, the process control is suggestive to aim at increasing acetic acid and ethyl acetate productions (Table 4) by carefully controlling the DO at initial phase (0–30 min) (Table 1) (Eq. 18).

In fact, such a chain type free radical reaction can be optimized as verified by Eqs. 31, 32, and 34. To enhance production of ethyl acetate and acetic acid would benefit the sensory aroma and taste. As can be seen from the finalized Eqs. 31 and 32, those are all functions of hydroxyl free radical concentration [·OH]. Obviously, to obtain good quality spirit, to carefully control the dissolved oxygen (DO) for optimization of the net formation rate of hydroxyl free radicals (Eq. 18) would be a crucial process-control strategy. Otherwise, the unwanted mineralization rate (Eq. 34) (Tables 1 and 2) has to be minimized.

Finally, cost analysis indicated that normally, an average of 6–7% per year can be saved (Table 7). In general, the sorghum young spirits need a minimum period of 4 years for aging before marketed. Thus, a total reduction of 24–28% can be expected for each batch.

In summary, the operational conditions for such photocatalyzed maturation technology are: an initial DO of 6.7 ppm in an effective reactor volume of 3 l which is dispersed with an amount of nanogold powder (80–120 nm, 6.6 mg/l) and installed with a built-in UV source (245 nm, 10 W). An optimum reaction time of 120 min at temperature <37°C and a percent degree of mineralization controlled at ≤4.87%. Under such a condition, the optimum ratio of [the favorable $(\text{esters}+\text{alcohols}+\text{ethers})_{\text{formed}}$]/[the favorable $(\text{acids})_{\text{formed}}$] ≥45.8 can be expected. Kinetic analysis has revealed that to obtain acetic acid and ethyl acetate that are favorable to the sensory taste of spirit, careful control of DO to attain an optimum production rate of hydroxyl free radical [·OH] can be a crucial step in the overall process. More importantly, this technology could provide advantages of container-saving, space-saving, labor-saving, and no storage-loss due to evaporation.

Conclusion

A novel nanogold photocatalyzed process has been developed, which when linked with biological ageing technology can accelerate maturity of young sorghum spirits. This technology could be an extremely cost-efficient innovation compared with the conventional process with respect to barrel-saving, space-saving, labor-saving, and storage-loss. Due to evaporation, kinetic equations have been developed by which an optimum control for production of main flavors and tastes, i.e., ethyl acetate and acetic acid, could be validated.

Acknowledgements The authors are thankful to the partial financial supports from Grants NHRI-EX95-91-6PN and DOH95-TD-B-11-002.

References

Amerine, M. A., & Ough, C. S. (1980). The Statistical Analysis of Failure Data. In J. D. Kalbfleisch, & R. L. Prentice. John Wiley & Sons, Inc., New York, USA.

Cantarelli, C. (1967). Fermentations et vinification 2nd Symoposium International d’Oenologie, Bordeaux-Cognac. pp 391–407é.

Cutzach, I., Chatonnet, P., & Dubourdieu, D. (1999). Study of the formation mechanisms of some volatile compounds during the aging of sweet fortified wines. *Journal of Agriculture Food and Chemistry*, *45*, 2837–2846.

Cutzach, I., Chatonnet, P., & Dubourdieu, D. (2000). Influence of storage conditions on the formation of some volatile compounds in white fortified wines (*Vins doux Naturels*) during the aging process. *Journal of Agriculture Food and Chemistry*, *48*, 2340–2345.

Escudero, A., Asensio, E., Cacho, J., & Ferreira, V. (2002). Sensory and chemical changes of young white wines stored under oxygen. An assessment of the role played by aldehydes and some other important odorants. *Food Chemistry*, *77*(3), 325–331.

Escudero, A., Cacho, J., & Ferreira, V. (2000b). Isolation and identification of odorants generated in wine during its oxidation: A gas chromatography-olfactometric study. *European Food Research and Technology*, *211*, 105–110.

Escudero, A., Hernandez-Orte, P., Cacho, J. E., & Ferreira, V. (2000a). Clues about the role of methional as character impact odorant of some oxidized wines. *Journal of Agriculture Food and Chemistry*, *48*, 4268–4272.

Ferreira, V., Escudero, A., Fernandez, P. E., & Cacho, J. E. (1997). Changes in the profile of volatile compounds in white wines stored under oxygen and their relationship with the browning process. *Z. Lebensm. Unters. Forsch.*, *205*, 392–396.

Izumi, I., Dunn, W. W., Wilbourn, K. O., Fan, F. F., & Bard, A. J. (1980). Heterogeneous photocatalytic oxidation of hydrocarbons on platinized TiO_2 powder. *Journal of Physical Chemistry*, *84*, 3207–3210.

Heller, S. R., & Miline, G. W. A. (1978a). *EPA/NIH Mass Spectral Data Base,* Vol 1. Washington DC: U.S. Government Printing Office.

Heller, S. R., & Miline, G. W. A. (1978b). *EPA/NIH Mass Spectral Data Base*, Suppl. 1. Washington DC: U.S. Government Printing Office.

International Organization for Standardization (ISO). (1987). Sensory Analysis: Methodology evaluation of food products by method using scales. International Standard —ISO 4121: Geneva, 7.

Majlat, P., Erdos, Z., & Takacs, J. (1974). Calculation and application of retention indices in programmed temperature gas chromatography. *Journal of Chromatography*, *91*, 89–103.

Maria Andre, B. H., Maurico, B., Ronaldo, F. N., Douglas, W. F., & Joao, B. F. (2004). Changes in the volatile composition in Brazilian sugar cane spirit during ageing in oak (Quercus spp.) casks. *Alimentaria (Alimentaria)*, *357*, 105–110.

Martínez, P., Codon, A. C., Pérez, L., & Benítez, T. (1995). Physiological and molecular characterization of flor yeasts: Polymorphism of flor yeast populations. *Yeast*, *11*, 1399–1411.

Ouyang, L. Y., & Chuang, B. R. (1999). A minimax distribution free procedure for inventory model subject to a service level constraint. *Journal of Interdisciplinary Mathematics*, *2*(1), 41–55.

Ouyang, L. Y., Chuang, B. R., & Wu, K. S. (1999). Optimal inventory policies involving variable lead time with defective items. *Opsearch*, *36*(4), 374–389.

Ouyang, L. Y., & Wu, K. S. (1999). Mixture inventory model involving variable lead time and defective units. *Journal of Statistics & Management Systems*, *2*(2–3), 143–157.

Peng, R. Y., Yang, T. C., Huang, W. K., & Juang, R. C. (1997). Photocatalytic sterilization by an UV-Zinc Oxide catalytic reactor. Proceedings of the Second Conference on Biochemical Engineering June 28 1997, Taipei 317–320.

Romer, G., & Renner, E. Z. (1974). Simple methods for isolation and concentration of flavor compounds from foods. *Z. Lebensm*, . *Unters. Forsch.*, *156*, 329–332.

Silva Ferreira, A. C., Guides de Pinho, P. G., Rdrigues, P., & Hogg, T. (2002). Kinetics of oxidative degradation of white wines and how they are affected by selected technological parameters 2002. *Journal of Agriculture Food and Chemistry*, *50*, 5919–5924.

Silva Ferreira, A. C., Hogg, T., & De Pinho, P. G. (2003). Identification of key odorants related to the typical aroma of oxidation-spoiled white wines. *Journal of Agriculture Food and Chemistry*, *51*, 1377–1381.

TNO (1981). *Compliation of mass spectra of volatile compounds in food*. The Netherlands: TNO Institute CIVO Analysis.

Turchi, C. S., & Ollis, D. F. (1990). Photocatalytic degradation of organic water contaminants: Mechanisms involving hydroxyl radical attack. *Journal of Catalysis*, *122*, 178–192.

Zoecklein, B. W., Fugelsang, K. C., Gump, B. H., & Nury, F. S. (1990). *Production Wine Analysis*. New York, U.S.A.: An AVI Book Published by Van Nostrand Reinhold.